Acta Crystallographica Section D
**Biological Crystallography**
ISSN 0907-4449

# Structure of diferric hen serum transferrin at 2.8 Å resolution

**Piyali Guha Thakurta, Debi Choudhury, Rakhi Dasgupta and J. K. Dattagupta***

Crystallography and Molecular Biology Division, Saha Institute of Nuclear Physics, 1/AF Bidhannagar, Kolkata 700 064, India

Correspondence e-mail: jiban@cmb2.saha.ernet.in

Received 4 April 2003
Accepted 28 July 2003

**PDB Reference:** hST, 1n04, r1n04sf.

Hen serum transferrin in its diferric form (hST) has been isolated, purified and the three-dimensional structure determined by X-ray crystallography at 2.8 Å resolution. The final refined structure of hST, comprising 5232 protein atoms, two $Fe^{3+}$ cations, two $CO_3^{2-}$ anions, 54 water molecules and one fucose moiety, has an $R$ factor of 21.5% and an $R_{free}$ of 26.9% for all data. The structure has been compared with the three-dimensional structure of hen ovotransferrin (hOT) and also with structures of some other transferrins, *viz.* rabbit serum transferrin (rST) and human lactoferrin (hLF). The overall conformation of the hST molecule is essentially the same as that of other transferrins. However, the relative orientation of the two lobes, which is related to the species-specific receptor-recognition property of transferrins, has been found to be different in hST from that in hOT, rST and hLF. On the basis of superposition of the N lobes, rotations of 5.8, 16.9 and 11.3° are required to bring the C lobes of hOT, rST and hLF, respectively, into coincidence with that of hST. A number of additional hydrogen bonds between the two domains in the N and C lobes have been identified in the structure of hST compared with that of hOT, which indicate a greater compactness of the lobes of hST than those of hOT. Being products of the same gene, hST and hOT have 100% sequence identity and differ only in the attached carbohydrate moiety. On the other hand, despite having similar functions, hST and rST have only 51% sequence similarity. However, the nature of the interdomain interactions of hST are closer to rST than to hOT. A putative carbohydrate-binding site has been identified in the N lobe of hST at Asn52 and a fucose molecule could be modelled at the site. The variations in interdomain and interlobe interactions in hST, together with altered lobe orientation with respect to hOT, rST and hLF, which are the representatives of the other subfamily of transferrins, are discussed.

## 1. Introduction

Transferrins are the major proteins involved in iron regulation and transport in vertebrates and some invertebrates (Aisen, 1989). The transferrin family is mainly subdivided into two branches: soluble glycoproteins and membrane melanotransferrins (Baker & Lindley, 1992). The soluble glycoproteins include serum transferrin found in blood, ovotransferrin found in avian egg white and lactoferrin found in numerous extracellular fluids and in the specific granules of polymorphonuclear lymphocytes. Serum transferrins transport iron from the blood stream to the cytosol in a pH-dependent manner by receptor-mediated endocytosis and lose their iron in mildly acidic media (Dautry-Varsat *et al.*, 1983). Ovotransferrins, which are identical to their avian serum

counterparts except for their attached carbohydrate, are assumed to be responsible for scavenging and transport of iron in egg white (Kurokawa *et al.*, 1995), whereas lactoferrins sequester iron from biological fluids and do not lose it in mildly acidic media (Montreuil *et al.*, 1960). These proteins are monomeric glycoproteins with a molecular weight of ~80 kDa, organized as two terminal lobes (N and C). The two lobes are endowed with a high degree of similarity and are assumed to arise from gene duplication; they are further divided into similarly sized domains NI and NII in the N lobe, and CI and CII in the C lobe. Each lobe contains an iron-binding cleft in which $Fe^{3+}$ is coordinated to the phenolate O atoms of two tyrosine residues, to the imidazole of a histidine residue, to the carboxylate of an aspartate residue and to a synergistic bicarbonate or carbonate adjacent to an arginine. It is generally believed that the two domains of each transferrin must open to allow the entry or release of $Fe^{3+}$. The iron-loaded holo form of the protein shows a higher affinity for the transferrin receptor than does the apo form, indicating that iron-dependent conformational changes may be important in the cellular uptake of iron (Young *et al.*, 1984; Mason *et al.*, 1987, 1996, 1997).

Both the avian transferrins, ovo and serum, are products of the same gene and have the same amino-acid sequence, differing only in their attached carbohydrate moiety (Thibodeau *et al.*, 1978). On the contrary, the sequence identity between hen serum transferrin and other mammalian serum transferrins, *e.g.* rabbit and porcine, is only 51%. All cell-binding studies (Mason *et al.*, 1987, 1996; Mason & Woodworth, 1984) have utilized ovotransferrin, with the assumption that it is identical to its serum counterpart, but an *in vivo* iron-transport function characteristic of serum transferrin has not been demonstrated for hOT (Mizutani, Muralidhara *et al.*, 2001). The fact that ovotransferrin does not have an iron-transport role may, however, be a consequence of its location in egg white. Also, *in vitro* studies have shown that while mammalian serum transferrin can utilize other mammalian transferrin receptors, ovotransferrin cannot do so (Shimo-oka *et al.*, 1986). Hence, it would be worthwhile to determine the three-dimensional structures of transferrins from different sources in order to understand the structural basis of their functions.

The structures of diferric forms of ovotransferrin have been determined at 2.4 Å for that from hen (Kurokawa *et al.*, 1995) and at 2.35 Å for that from duck (Rawas *et al.*, 1996). Crystal structures of intact apo ovotransferrin have been solved at 3.0 Å for that from hen (Kurokawa *et al.*, 1999) and at 4.0 Å for that from duck (Rawas *et al.*, 1989). Several high-resolution crystal structures are available for half-molecules of the apo and holo forms of hen ovotransferrin (Lindley *et al.*, 1993; Mizutani *et al.*, 1999, 2000; Mizutani, Muralidhara *et al.*, 2001; Mizutani, Mikami *et al.*, 2001; Kuser *et al.*, 2002). A number of structures of the intact molecules of the apo and holo forms of lactoferrins have also been determined (Haridas *et al.*, 1995; Moore *et al.*, 1997; Sharma, Paramasivam *et al.*, 1999; Karthikeyan *et al.*, 1999; Jameson *et al.*, 1998; Khan *et al.*, 2001; Sharma, Rajashankar *et al.*, 1999).

On the other hand, only two structures of intact serum transferrin (Bailey *et al.*, 1988; Hall *et al.*, 2002) have been solved so far. In addition to these, some structures of half-molecules of recombinant human serum transferrin (MacGillivray *et al.*, 1998; Jeffrey *et al.*, 1998; Bewley *et al.*, 1999; Nurizzo *et al.*, 2001) are available. These structures lack information about the structural differences related to functional properties between the mammalian serum transferrins and avian serum transferrins. As a result, the differences in iron binding and release between the species and classes of serum transferrins are still poorly understood. No complete structure or structure of part of an avian serum transferrin in either the apo or holo form has yet been reported. Hence, in order to investigate the structural basis of the variations in the iron-binding and iron-release properties of serum transferrins of different species and also to address the diversities in their receptor-binding properties, comparison of the detailed crystallographic structures is important. Here, we report the crystal structure of diferric hen serum transferrin (hST) at 2.8 Å resolution. We have compared the hST structure with the diferric forms of hen ovotransferrin (hOT; PDB code 1ovt), rabbit serum transferrin (rST; PDB code 1jnf) and human lactoferrin (hLF; PDB code 1lfg), which are representatives of each subfamily of soluble transferrins.

## 2. Experimental

### 2.1. Isolation and purification

Serum was extracted from the blood of ovulating white leghorn birds and was kept frozen at 253 K. Serum transferrin in its apo form was isolated and purified from the serum by hydrophobic interaction chromatography using phenyl Sepharose CL 4B (Sigma, MO, USA) according to a previously reported method (Choudhury *et al.*, 2002). To obtain the holo form, the purified protein was first dialyzed exhaustively against 100 m*M* citrate–bicarbonate buffer pH 8.0 and then saturated with iron by incubating it with $FeCl_3$ at 293 K at a protein:$FeCl_3$ ratio of 1:2. Excess iron was removed by dialyzing the iron-saturated protein against distilled water, which was maintained at pH 8.0. This protein was then concentrated using Ultrafree-MC filter units (Sigma) and used for crystallization experiments.

### 2.2. Crystallization

All crystallization experiments were performed using the hanging-drop vapour-diffusion method. Initial attempts to crystallize diferric hen serum transferrin with commercially available sparse-matrix screening kits, Crystal Screens I and II from Hampton Research, were unsuccessful. Good diffracting crystals were obtained under two conditions: (i) 17–20% PEG 6000 in 20 m*M* sodium acetate buffer pH 6.0 and (ii) 18–21% PEG 4000 in 40 m*M* sodium cacodylate buffer pH 5.9 containing 20 m*M* $NaHCO_3$. The protein concentration used for crystallization was ~40 mg ml$^{-1}$ (in 40 m*M* sodium cacodylate buffer pH 5.9). The hanging drops were set up by mixing equal volumes of protein and precipitant on siliconized

**Table 1**
Summary of diffraction data collection.

Values in parentheses correspond to the outermost resolution shell.

| | |
|---|---|
| Space group | $P2_1$ |
| Unit-cell parameters (Å, °) | $a$ = 72.96, $b$ = 59.11, $c$ = 81.86, $\beta$ = 95.6 |
| Temperature (K) | 100 |
| $V_M$ (Å$^3$ Da$^{-1}$) | 2.23 |
| Molecules per AU | 1 |
| Total No. of reflections | 155917 |
| No. of unique reflections | 17301 |
| Resolution (Å) | 2.8 (2.86–2.80) |
| Average $I/\sigma(I)$ | 9.7 (2.1) |
| Completeness (%) | 92.3 (92.4) |
| $R_{merge}$ † | 0.08 (0.37) |

† $R_{merge} = \sum[(I - \langle I\rangle)^2]/\sum(I^2)$.

cover slips and equilibrating them against the precipitant solution at 277 K. The thin needle-shaped deep red coloured holo form crystals grew within two weeks. The crystal used for X-ray data collection was obtained using condition (ii).

### 2.3. Diffraction data collection and processing

Prior to data collection, individual crystals were cryo-protected by equilibrating them for a few seconds in 25–30% MPD solution prepared in reservoir solution. The crystal was then directly flash-frozen and maintained at 100 K during the entire data collection using an Oxford Cryosystems cooling unit. X-ray intensity data were collected to 2.8 Å resolution using a 30 cm MAR Research image-plate detector with Cu $K\alpha$ radiation from a Rigaku RU-200 rotating-anode generator equipped with Osmic MaxFlux confocal optics and running at 50 kV and 90 mA. A total of 138 frames were recorded with an oscillation angle of 1.0°, a crystal-to-detector distance of 150 mm and an exposure time of 8 min per image. The X-ray diffraction data were indexed, integrated and subsequently scaled using *DENZO* and *SCALEPACK* from the *HKL* program package (Otwinowski & Minor, 1997). A summary of diffraction data collection is given in Table 1.

### 2.4. Structure solution and refinement

The structure of diferric hen serum transferrin was solved by the molecular-replacement method with the program *AMoRe* (Navaza, 1994) as implemented in the *CCP*4 suite (Collaborative Computational Project, Number 4, 1994) using the coordinates of diferric hen ovotransferrin (PDB code 1ovt) as the starting model. The rotation and translation functions were calculated with X-ray data in the resolution range 10.0–4.0 Å, which gave an unambiguous solution with a correlation factor of 49.7% and an $R$ factor of 42.8%. Rigid-body refinement using *AMoRe* reduced the $R$ value to 40.9%. The model was subjected to further refinement as six rigid bodies (residues 4–94, 95–249, 250–333, 344–430, 431–591 and 592–686 with hOT numbering) in *CNS* (Brünger *et al.*, 1998), delineating the domain organization of serum transferrin, in the resolution range 20.0–2.8 Å, which resulted in $R$ and $R_{free}$ values of 36.6 and 35.4%, respectively. Subsequent refinement steps were carried out using *CNS*. A random sample of 5% of reflections in the data set were excluded from the refinement and used for $R_{free}$ calculation. Manual fitting of the model to the $2F_o - F_c$ electron-density map was performed using the interactive graphics package *O* (Jones *et al.*, 1991). The first three amino-acid residues from the N-terminus were omitted from the structure owing to lack of electron density and 16 residues for which no side-chain electron density was observed were truncated to Ala. The model was further refined by simulated annealing with molecular dynamics using a slow-cooling protocol similar to that of Brünger *et al.* (1989) from 3000 to 300 K, which lowered the $R$ and $R_{free}$ values to 26.0 and 30.1%, respectively. The quality of the electron-density map improved considerably at this stage. Manual rebuilding was again performed with *O*. Two iron and bicarbonate ions were fitted in the $F_o - F_c$ electron-density map contoured at the 3.0$\sigma$ level. After a few cycles of positional refinement alternating with model refitting into the map, the $R$ and $R_{free}$ values decreased to 24.1 and 28.2%, respectively. At this stage, 54 water molecules were incorporated in the model conservatively, *i.e.* only if they appeared as discrete spherical peaks in both $2F_o - F_c$ and $F_o - F_c$ electron-density maps at levels above 1.0$\sigma$ and 3.0$\sigma$, respectively, and satisfied the hydrogen-bonding criteria. Careful inspection of the map revealed extra interpretable electron density next to the side chain of Asn52. A fucose molecule was modelled at this site, taking coordinates from the HIC-UP (Kleywegt & Jones, 1998) library, and could be fitted in the $F_o - F_c$ electron-density map at 3.0$\sigma$. After occupancy refinement of the modelled fucose molecule, no negative peak was found at this position. Subsequent positional and $B$-group refinement of the structure finally converged to a final $R$ factor of 21.6% and an $R_{free}$ of 26.9%. A summary of the final refinement statistics is given in Table 2. The mean temperature factor for all protein atoms was found to be 39.8 Å$^2$. The root-mean-square deviations from standard bond lengths and angles are 0.007 Å and 1.5°, respectively.

**Table 2**
Summary of refinement statistics.

| | |
|---|---|
| Resolution limits (Å) | 15.0–2.8 |
| No. of reflections in working set | 14925 |
| No. of reflections in test set | 768 |
| No. of protein atoms | 5232 |
| No. of solvent molecules | 54 |
| Other ions | $2Fe^{3+}$, $2CO_3^{2-}$ |
| No. of carbohydrate atoms | 11 |
| Final $R$ factor (%) | 21.6 |
| $R_{free}$ (%) | 26.9 |
| Average $B$ factor (Å$^2$) | 39.8 |
| Residues truncated to alanine | Lys179, Gln335, Leu336, Thr337, Ser339, Arg341, Glu342, Glu418, Lys423, Asp425, Glu426, Lys439, Leu501, Asp556, Lys559, Lys646 |
| R.m.s. deviation from ideal geometry | |
| Bond distance (Å) | 0.007 |
| Bond angles (°) | 1.5 |
| Dihedral angles (°) | 23.6 |
| Improper dihedrals (°) | 0.86 |
| Ramchandran statistics (%) | |
| Most favourable | 78.9 |
| Additionally allowed | 18.9 |
| Generously allowed | 1.5 |
| Disallowed | 0.7 |

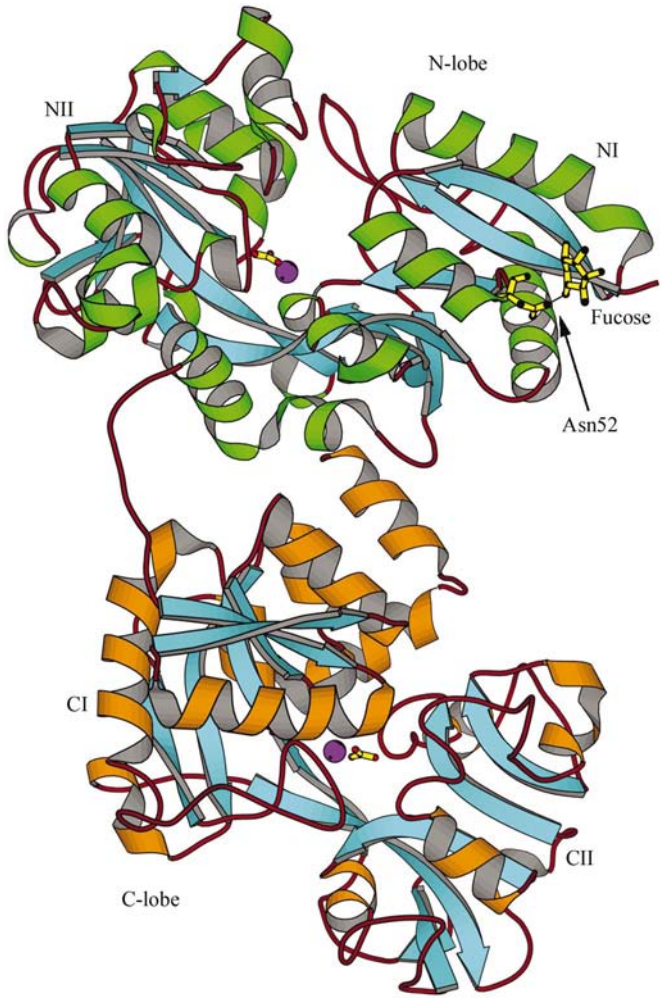


**Figure 1**
Crystallographic structure of diferric hen serum transferrin (hST), showing the lobe and domain delineation and the secondary-structure elements. The Fe atoms are shown as purple-coloured spheres and the carbonate is in a ball-and-stick presentation. Asn52 and the modelled fucose molecule attached to it are indicated. The diagram was generated using *MOLSCRIPT* (Kraulis, 1991).

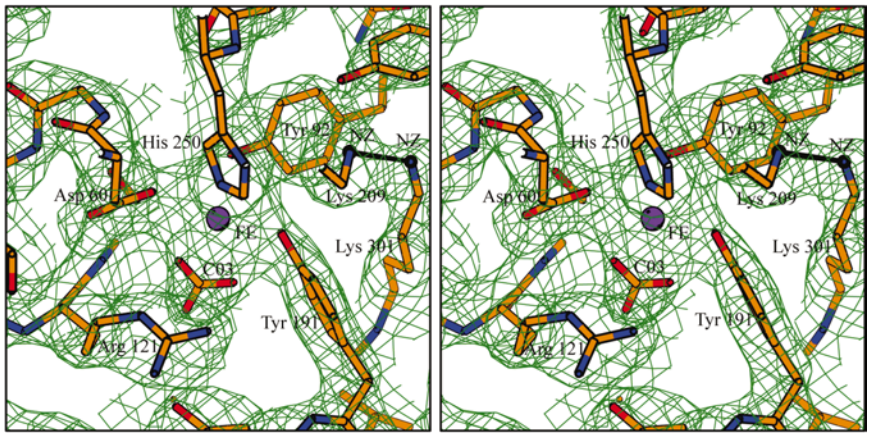


**Figure 2**
Stereoview of the electron-density map ($2F_o - F_c$) contoured at 1.0$\sigma$ around the iron-binding region together with the dilysine trigger of the hST structure. The distance between the NZ atom of Lys209 and the NZ atom of Lys301 is 2.5 Å. The diagram was generated using *BOBSCRIPT* (Esnouf, 1997).

The program *PROCHECK* (Laskowski *et al.*, 1993) was used to check the stereochemical quality of the structure. The Ramchandran plot of the main-chain torsion angles shows that 99.3% of the residues lie within the allowed region (Table 2). Four residues were found to be in the disallowed region, of which two are Leu299 and Leu636, which are involved in the conserved $\gamma$-turn in each lobe. The other two disallowed residues are Ser339 and Arg341 (both truncated to Ala), which lie in the region of the linker peptide that connects the two lobes. From a Luzzati plot, the mean absolute error in atomic positions was estimated to be 0.34 Å. The final model of diferric hen serum transferrin (hST) consists of 683 amino-acid residues, two $Fe^{3+}$ ions, two $CO_2^{3-}$ ions, 54 water molecules and one modelled fucose residue.

## 3. Results and discussion

### 3.1. Overall organization of the structure

Members of the transferrin family show a high level of sequence identity (Baker, 1994), which is translated into similar polypeptide-chain folding. The overall conformation of the polypeptide chain of hST (Fig. 1) is essentially the same as other members of the transferrin family. Briefly, the molecule is split into two homologous N and C lobes. The lobes are further divided into two similarly sized domains: NI and NII in the N lobe, and CI and CII in the C lobe. The two $Fe^{3+}$-binding sites are located in the interdomain clefts of each lobe. In the N lobe, domain NI comprises residues 4–94 and 250–333, and domain NII comprises residues 95–249. Similarly, in the C lobe, domain CI is composed of residues 344–430 and 592–686, and CII is composed of residues 431–591. The two domains are linked by two antiparallel $\beta$-strands that form the hinge region about which domain II pivots in order to give the open form of the apo protein. The residues that comprise the hinge region in the N lobe are residues 89–94 and 244–249. Presumably, the corresponding residues 429–435 and 586–592 in the C lobe will constitute the hinge region. The superposition of the C-terminal lobe on the N-terminal lobe of hST gives an r.m.s. deviation of 1.5 Å with 287 equivalent $C^{\alpha}$ atoms and requires a rotation of 176.0° around a screw axis followed by a translation of 24.8 Å. When the N lobe of hST was independently superimposed on the N lobes of hOT, rST and hLF, the r.m.s. deviations of the $C^{\alpha}$ atoms were found to be 0.5, 1.1 and 1.0 Å, respectively, while for the C lobes the values were 0.8, 1.1 and 1.1 Å, respectively.

The assignment of secondary-structural elements and the three-dimensional arrangement for hST are shown in Table 3 and Fig. 1. The nomenclature used in defining the secondary structure is that described by Kurokawa *et al.* (1995) for hOT. In the secondary structure of hST, most of the corresponding helices in the N

**Table 3**
Secondary-structure assignment in hen serum transferrin.

| N-lobe residues | Nomenclature | C-lobe residues |
|---|---|---|
| Helices | | |
| 13–27 | 1 | 351–365 |
| 41–51 | 2 | 376–386 |
| 60–68 | 3 | 395–405 |
| 106–108 | 4 | |
| 121–135 | 5 | 464–475 |
| 147–156 | 6 | 480–484 |
| 167–172 | 6a | 496–500 |
| 189–200 | 7 | 523–533 |
| | 7a | 543–549 |
| 217–222 | 8a | 557–561 |
| 235–242 | 8b | |
| | 8c | 597–599 |
| 258–275 | 9 | 600–616 |
| 292–296 | 9a | |
| 315–321 | 10 | 652–658 |
| 321–331 | 11 | |
| | 12 | 674–684 |
| $\beta$-strands | | |
| 5–12 | *a* | 345–350 |
| 33–39 | *b* | 368–375 |
| 57–59 | *c* | 392–394 |
| 75–83 | *d* | 408–414 |
| 90–100 | *e* | 429–439 |
| 114–117 | *f* | 451–455 |
| 158–160 | *g* | 486–488 |
| 205–210 | *h* | 537–542 |
| 223–228 | *i* | 565–570 |
| 232–234 | *i*1 | 574–576 |
| 245–254 | *j* | 586–596 |
| 303–310 | *k* | 643–647 |

and C lobes are identical except for a few changes: (i) helix 6 in the C lobe is shortened by five residues, (ii) helices 7a and 8c are not observed in the N lobe, whereas helices 8b and 9a are not found in the C lobe, (iii) helix 11 (residues 321–331), which appears to stabilize the closed conformation of transferrins by making contact with helix 5 in the N lobe, has no corresponding helix in the C lobe of hST and (iv) the inter-lobe bridging peptide (residues 332–342) which corresponds to helix 12 of the C lobe is in an extended conformation. Helices 3 and 5 are important for metal and anion binding. The nature of helices 3 and 5 are unchanged from that of hOT. There are two helices in the N lobe of hOT (211–217 and 444–448) which are missing in hST, whereas two other helices (235–242 and 292–296) which have been observed in hST are not present in hOT. In the C lobe, there is an extra helix (597–599) that is absent in hOT. When the helices of hST are compared with those of rST and hLF, it is found that the majority of them are unchanged except the interlobe-connecting peptide. This peptide is a helix in hLF and an extended loop in hST and rST. We have identified 12 $\beta$-strands in hST which are similar to those found in hOT and rST, whereas hLF has one strand less. The difference in the structure of these strands is either deletion or insertion of one or two residues in some of them. The $\beta$-sheet in the NI and CI domain contains strands *a*, *b*, *c* and *d* which point towards the interdomain cleft, and strands *j* and *k* pointing away from the cleft. Similarly, the $\beta$-sheet in the NII and CII domains include strands *f*, *g*, *h* and *i* oriented towards the interdomain cleft, and strands *e* and *i*1 pointing away from the cleft. Two *cis*-proline residues that have been

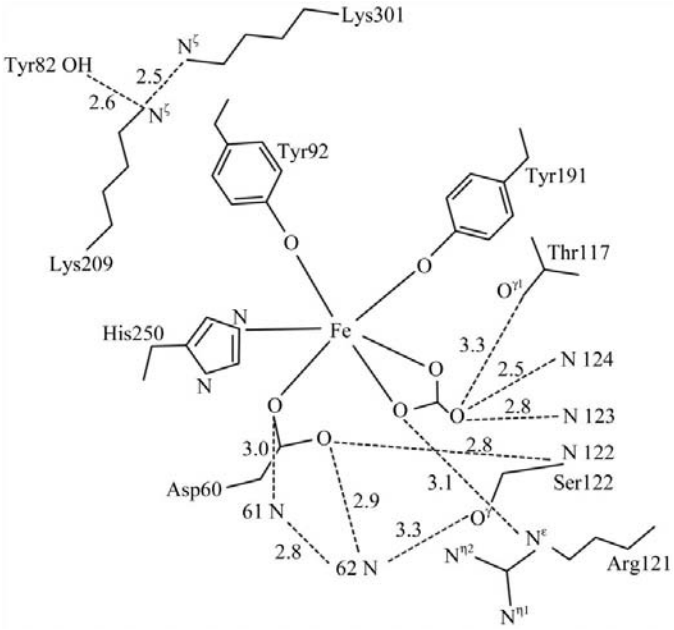


**Figure 3**
Schematic diagram of the coordination environment and the hydrogen-bonding network around $Fe^{3+}$ and the dilysine trigger in the N lobe of hST. The hydrogen-bond lengths are indicated in Å.

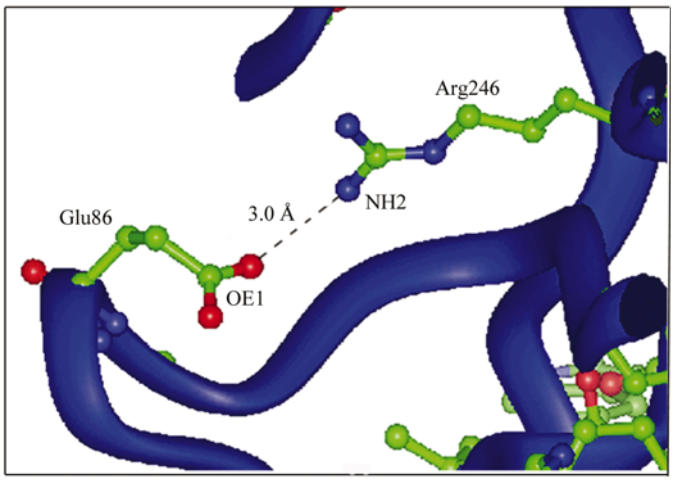


**Figure 4**
The unique interdomain salt bridge between Glu86 and Arg246 in the N lobe. The figure was generated with *Insight*II (MSI Inc.)

identified in the present structure are 71 and 287. Thus, comparison of secondary structures of hST and hOT reveals there to be some differences in the organization of the helices of the two proteins. These differences may be important, since these helices are involved in stabilizing the iron-binding site and the closed conformation of the proteins to some extent.

### 3.2. Nature of metal- and anion-binding sites

The conserved nature of the metal- and anion-binding sites in all transferrins demonstrates the extent to which these sites are optimized for binding of $Fe^{3+}$ and $CO_3^{2-}$; in all cases, both the identity of the ligands and their geometrical arrangement is the same. The binding sites in the present hST structure

**Table 4**
Geometry of the iron- and anion-binding sites of hen serum transferrin.

| | N lobe | C lobe |
|---|---|---|
| Bond lengths (Å) | | |
| Fe—$O^{\delta1}$ 60 (395) | 2.3 | 2.1 |
| Fe—OH 92 (431) | 2.2 | 2.3 |
| Fe—OH 191 (524) | 2.1 | 2.1 |
| Fe—$N^{\varepsilon}$ 250 (592) | 2.2 | 1.9 |
| Fe—O1 | 2.2 | 2.1 |
| Fe—O2 | 1.9 | 2.0 |
| Bond angles (°) | | |
| $O^{\delta1}$ 60 (395)—Fe—OH 92 (431) | 80.4 | 93.0 |
| $O^{\delta1}$ 60 (395)—Fe—OH 191 (524) | 167.9 | 163.3 |
| $O^{\delta1}$ 60 (395)—Fe—$N^{\varepsilon}$ 250 (592) | 78.6 | 68.4 |
| $O^{\delta1}$ 60 (395)—Fe—O1 | 125.4 | 81.0 |
| $O^{\delta1}$ 60 (395)—Fe—O2 | 68.7 | 94.4 |
| OH 92 (431)—Fe—OH 191 (524) | 92.6 | 102.1 |
| OH 92 (431)—Fe—$N^{\varepsilon}$ 250 (592) | 77.4 | 89.7 |
| OH 92 (431)—Fe—O1 | 139.0 | 162.9 |
| OH 92 (431)—Fe—O2 | 142.3 | 98.8 |
| OH 191 (524)—Fe—$N^{\varepsilon}$ 250 (592) | 90.4 | 117.8 |
| OH 191 (524)—Fe—O2 | 121.3 | 76.8 |
| OH 191 (524)—Fe—O1 | 66.0 | 82.6 |
| $N^{\varepsilon}$ 250 (592)—Fe—O2 | 115.2 | 161.3 |
| $N^{\varepsilon}$ 250 (592)—Fe—O1 | 133.7 | 102.8 |
| O2—Fe—O1 | 58.1 | 66.0 |

have a distorted octahedral coordination similar to other transferrins, involving a bidentate synergistic carbonate anion and four protein ligands, namely the phenolate O atoms of Tyr92 and Tyr191, the $N^{\varepsilon2}$ imidazole N atom of His250 and a carboxylate O atom of Asp60 in the N lobe and the corresponding atoms of Tyr431, Tyr524, His592 and Asp395 in the C lobe. Tyr92 (431), Asp60 (395) and His250 (592) are contributed by domain I, of which Tyr92 (431) comes from the hinge region, while Tyr191 (524) belongs to domain II. The anion is held in place by Arg121 (460) and Thr117 (456), which belong to domain II. It has been shown by mutagenesis that changing any one of the protein ligands involved in iron binding destabilizes the site, resulting in alterations in the iron-binding properties (Woodworth *et al.*, 1991). The electron density contoured at 1.0$\sigma$ and the interactions surrounding this iron-binding site in the N lobe of hST are illustrated in Figs. 2 and 3, while the details of the geometry are given in Table 4. The two bound Fe atoms are 43.5 Å apart, which is comparable to their distance in hOT, rST and hLF. A few distinguishing features have been observed in this site of hST compared with those of hOT, rST and hLF. The synergistic binding of the anion in transferrins requires an intact helix 5 and correct positioning of Arg121 to partially neutralize the positively charged groups in the iron-binding cleft. In hST, only $N^{\varepsilon}$ of Arg121 (460) is involved in carbonate bonding, whereas in hOT, in addition to $N^{\varepsilon}$, $N^{\eta2}$ is also involved in bonding to carbonate. As a consequence, Arg121 is probably loosely bonded to the carbonate anion in hST compared with hOT. In hST, the non-ligating O atom, $O^{\delta2}$ of Asp60 (395) forms hydrogen bonds with main-chain N atoms of Ser122 (Thr461) and Gly62 (397). On the other hand, Gly62 N also forms a hydrogen bond with Ser122 $O^{\gamma}$. In the C lobe, the hydrogen bond formed between Gly397 N and Thr461 $O^{\gamma1}$ is weaker (3.4 Å) compared with that in hOT (2.98 Å). Hence, Ser122 $O^{\gamma}$ (Thr in hLF) does not interact directly with Asp60 $O^{\delta2}$ in hST as observed in hOT, rST and hLF. Since Asp60 (395) is implied in domain opening and closure, this difference in interaction is likely to affect the domain motion of hST.

### 3.3. Interdomain interactions

A feature common to all transferrins is the closing of the interdomain clefts upon incorporation of iron into the ion-binding sites (Grossmann *et al.*, 1991), leading to a more compact structure of the protein molecule which may be necessary to prevent hydrolysis of the bound iron. The external factors which appear to influence the iron binding and stability are the interdomain and interlobe interactions. The binding cleft of each lobe is predominantly polar in nature and is formed by the inner surfaces of its two domains. Apart from the bonding of the $Fe^{3+}$ and $CO_3^{2-}$ ions and the ligating amino acids, the hydrogen bonds formed between the residues of the two domains surrounding the iron-binding cleft constitute the interdomain interactions involved in domain movements. We have identified 11 interdomain interactions in the N lobe and ten in the C lobe of hST (Table 5). The number of interdomain interactions in the N lobe of hOT, rST and hLF are eight, ten and eight, respectively, while those in the C lobe of these proteins are six, 14 and five, respectively (Kurokawa *et al.*, 1995; Hall *et al.*, 2002; Haridas *et al.*, 1995). Hence, the number of interdomain interactions in both the lobes of hST molecule is comparable to that in serum transferrin rather than that in ovotransferrin. Interactions 3, 4 and 5 (Table 5) in the N lobe and interactions 1, 5–8, 10 and 11 in the C lobe of hST are different from those in the corresponding lobes of hOT. Two interdomain salt bridges, Lys290 $N^{\zeta}\cdots$Asp219 $O^{\delta2}$ and Glu86 $O^{\varepsilon1}\cdots$Arg246 $N^{\eta2}$, have been identified at the tip of the cleft in the N lobe and are at a distance of ∼20 Å from the iron-binding site. The second salt bridge, shown in Fig. 4, has not been observed in either hOT, rST or hLF. The N lobe of rST does not include any salt bridge, whereas hLF has two salt bridges. The hydrogen bond Asn632 $N^{\delta2}\cdots$Glu547 O in the C lobe of hOT is replaced by Asn632 $N^{\delta2}\cdots$Lys552 O in hST, which also lies at the mouth of the interdomain cleft. Asn632 O makes a hydrogen bond with Thr525 $O^{\gamma1}$ which is absent in hOT. The presence of a larger number of hydrogen bonds in the C lobe of hST compared with that of hOT would make the closed conformation of this lobe more stable. The three conserved hydrogen bonds implicated in the hinge motion in the N lobe of the hen ovotransferrin structure determined at 1.65 Å (Mizutani, Mikami *et al.*, 2001) are also found to be present in the present 2.8 Å structure of hST. In addition to these, we have identified one further hydrogen bond between Tyr93 OH and Arg246 $N^{\eta1}$ in this region. A similar hydrogen-bonding network has been observed in the C lobe amongst the corresponding residues implicated in the hinge motion of this lobe.

Thus, the numbers and types of interactions present in the N and C lobes of hST are more similar to rST than to hOT or hLF. These observations indicate a difference in the interdomain hydrogen-bonding network of serum transferrins compared with ovotransferrins and lactoferrins. The present

**Table 5**
Interdomain hydrogen bonds and salt bridges in hST.

All distances ≤3.3 Å are given. The dilysine trigger is shown in bold and salt bridges are in italics.

| No. | Domain NI | Domain NII | Distance (Å) | Domain CI | Domain CII | Distance (Å) |
|---|---|---|---|---|---|---|
| 1 | Asp60 $O^{\delta2}$ | Ser122 N | 2.8 | Lys352 N | His518 $N^{\epsilon2}$ | 3.0 |
| 2 | Gly62 N | Ser122 $O^{\gamma}$ | 3.3 | Asp353 $O^{\delta2}$ | Ser517 $O^{\gamma}$ | 2.5 |
| 3 | ***Glu86 $O^{\epsilon1}$*** | ***Arg246 $N^{\eta2}$*** | ***3.0*** | Asp395 $O^{\delta1}$ | Thr461 $O^{\gamma1}$ | 3.3 |
| 4 | Tyr93 N | His210 $N^{\delta1}$ | 3.1 | Asp395 $O^{\delta2}$ | Thr461 N | 2.8 |
| 5 | Tyr93 O | His210 N | 2.8 | Glu413 O | Thr591 $O^{\gamma1}$ | 2.4 |
| 6 | Ser122 $O^{\gamma}$ | Tyr324 OH | 2.7 | Tyr415 OH | Thr591 $O^{\gamma1}$ | 3.1 |
| 7 | Asn126 $N^{\delta2}$ | Tyr324 OH | 3.0 | Tyr524 OH | Lys638 $N^{\zeta}$ | 3.0 |
| 8 | **Lys209 $N^{\zeta}$** | **Lys301 $N^{\zeta}$** | **2.5** | Tyr525 $O^{\gamma1}$ | Asn632 O | 2.5 |
| 9 | Glu215 O | Lys296 $N^{\zeta}$ | 2.5 | ***Gln541 $O^{\epsilon1}$*** | ***Lys638 $N^{\zeta}$*** | ***3.3*** |
| 10 | Asn216 $O^{\delta1}$ | Lys296 $N^{\zeta}$ | 2.6 | Lys552 O | Asn632 $N^{\delta2}$ | 3.1 |
| 11 | ***Asp219 $O^{\delta2}$*** | ***Lys290 $N^{\zeta}$*** | ***3.0*** | | | |

study also reveals that the serum transferrins (hST, rST and pST) contain a larger number of interdomain interactions than either ovotransferrin (hOT) or lactoferrin (hLF). Hence, it may be inferred that the lobes of serum transferrins are intrinsically more stable.

All the hydrogen bonds in the structure were detected using the program *CONTACT* implemented in the *CCP*4 suite of programs (Collaborative Computational Project, Number 4, 1994) as interactions with donor-to-acceptor atom distances within 3.3 Å and the bond angle formed by the donor atom, acceptor atom and the atom attached to the acceptor atom was between 90 and 120°.

### 3.4. Dilysine trigger

Apart from the possible protonation of a histidine ligand, the existence of a pH-sensitive 'trigger' involving a hydrogen-bonded pair of lysines in the N lobe of serum and ovotransferrins is related to the release of the bound iron at low intracellular pH (Dewan *et al.*, 1993). It has been observed in the case of human transferrin that the mutation H249E results in the abolition of the dilysine trigger, causing the mutant to release iron about three times faster than the wild type and causing an increase in the acid stability of the protein (MacGillivray *et al.*, 2000). In general, it is more likely that protonation of the coordinated histidine (Jeffrey *et al.*, 1998) and the carbonate anion (El Hage Chahine & Pakdaman, 1975; MacGillivray *et al.*, 1998) will constitute the initial stages, but the dilysine trigger may then be important when the iron coordination has been weakened. This dilysine trigger in hST (Figs. 2 and 3) is located immediately behind the iron-binding site at about 6.0 Å from the Fe atom. The distance between Lys209 $N^{\zeta}$ and Lys301 $N^{\zeta}$ in the present structure is 2.5 Å, whilst the corresponding distances in hOT and rST are 2.9 and 2.5 Å, respectively. Hence, the Lys–Lys distance observed here at the present resolution is comparable to a serum transferrin rather than an ovotransferrin. In addition to the Lys–Lys interaction, Lys209 $N^{\zeta}$ also forms a weak hydrogen bond with Ser303 $O^{\gamma}$ (3.4 Å), which is another interdomain interaction present in the N lobe of hST. The $N^{\zeta}$ atom of Lys301 makes a hydrogen bond with Tyr82 OH (2.6 Å). Although a similar couple is present at an equivalent position in the C lobe, one of the lysine residues (Lys638) is replaced by a glutamine (Gln541) in this lobe and the distance between the $N^{\zeta}$ atom of Lys638 and the $O^{\epsilon1}$ atom of Gln541 is 3.3 Å. The environment of both the Lys–Lys couple and the Gln–Lys couple is hydrophobic in nature, similar to that in hOT, being surrounded by Tyr82 (415), Tyr92 (431) and Tyr191 (524).

### 3.5. Interlobe interactions and lobe orientation

As is well known, the major structural difference between the transferrins is the relative orientation of the two lobes and the extent of domain closure. Studies of the binding of ovotransferrin C lobe to the N lobe using titration calorimetry showed clearly that both the free energy and heat of interaction of the two half-molecules were dependent on whether neither, one or both had an attached ferric ion (Lin *et al.*, 1991). Also, both the N and C lobes of ovotransferrin contain recognition sites that are required to attain physiological levels of binding and their pre-association is required for full binding to the chicken transferrin receptor (Mason *et al.*, 1996). It has been observed that while intact N-terminal and C-terminal half-molecule fragments of hOT associate to form an N–C dimer, the N- and C-terminal fragments of hOT in which the residues 320–332 and 683–686 are removed by proteolytic digestion are unable to associate (Williams & Moreton, 1988). In hST, as in other transferrins, two elements mainly link the two lobes: the covalent connection provided by the bridging peptide and the hydrophobic 'cushion' formed by the packing of non-polar surfaces on both the lobes. The residues involved in the interactions between two lobes in hST are 308–323, which are contributed by helices 10 and 11, together with the preceding loop 311–314 and residues 87–89 in the N lobe, while in the C-lobe the residues which participate in the interlobe contacts are 386 and 676–686 from helix 12. The interlobe interactions are mostly hydrophobic in nature and the contributing residues are Lys308, Pro311, Leu313, Met314, Leu318 in the N lobe, and Lys386, Ile676, Met679, Phe682 and Leu683 in the C lobe. The interactions between the residues of the N lobe and the terminating helix of the C lobe are one of the major contributors towards the stability of the whole molecule. Other specific interactions between the two lobes include one salt bridge, Asp315 $O^{\delta1}\cdots$Lys386 $N^{\zeta}$.

The differences in the relative orientations of the two lobes of various transferrins have been attributed to differences in the conformation of the interlobe-connecting peptides (Kurokawa *et al.*, 1995). On superposition of the hST and hOT structures, the r.m.s. deviations of $C^{\alpha}$ atoms were found to vary greatly in the region 332–342, which is the bridging peptide. The conformation of this peptide was also found to be altered from that of hOT as seen from the large changes in the main-chain dihedral angles. If the N lobes of hST and hOT are superimposed, a rotation of 5.8° followed by a translation of

0.8 Å is required to match the C lobes (Fig. 5*a*). If the N lobes of rST and hLF are superimposed on the N lobe of hST, rotations of 16.9° (Fig. 5*b*) and 11.3° with translations of 0.5 and 0.8 Å are required to bring the C lobes into coincidence. The difference in the lobe orientations of hOT and rST was found to be 6.8° (Kurokawa *et al.*, 1995). Therefore, the difference in the lobe orientation between mammalian serum transferrin (rST) and avian serum transferrin (hST) is large compared with that between avian ovotransferrin (hOT) and avian serum transferrin (hST) as well as between avian ovotransferrin (hOT) and mammalian serum transferrin (rST). Thus, the differences in the lobe orientations can be correlated with the species-specific receptor-recognition property of transferrins.

### 3.6. Carbohydrate structure

All transferrins are glycosylated, although there appears to be no significant functional role of the carbohydrate moieties with respect to iron metabolism since they are widely distributed on the protein surface in differing numbers in different transferrins (Baker & Lindley, 1992). Most of the time, the carbohydrates are ill-defined beyond the first two or three sugars. The carbohydrate-attachment sites in transferrins often vary in different species, but one site, Asn473 (in hOT and hST, and the equivalent Asn in other transferrins), is conserved. It has been reported previously that there is more than one type of carbohydrate moiety present in hST/hOT (Williams, 1968). No carbohydrate moiety was found in the holo structure of hen ovotransferrin, but two core GlcNac residues were located in the corresponding apo structure which were postulated to contribute to the stability of the open form of the protein (Kurokawa *et al.*, 1999). Based on the sequence, two possible carbohydrate-binding sites were proposed to be present in the porcine serum transferrin structure and a second binding site was subsequently identified at Asn25 of the N lobe (Hall *et al.*, 2002). One of the possible reasons for this may be the presence of more than one carbohydrate-binding site on the protein. Although no electron density was found attached to Asn473 in hST, an interpretable ring-like electron density ($F_o - F_c$ map, contoured at a level of 3.0$\sigma$) was observed to be attached to Asn52. We modelled a fucose molecule there (Fig. 1) which fitted well in this density. Hence, we postulate that Asn52 may be a second putative site of carbohydrate attachment in hST.

It has been suggested that attachment of carbohydrate to proteins lowers the overall thermal motion of the protein molecule and also reduces its susceptibility to proteolysis and thermal denaturation (Rudd *et al.*, 1994; Mer *et al.*, 1996; Wang *et al.*, 1996). The possibility of Asn52 as a second putative site of carbohydrate attachment in hST, however, needs to be explored by obtaining a higher resolution structure and the exact nature of the carbohydrate needs to be confirmed further by mass-spectroscopic analysis.

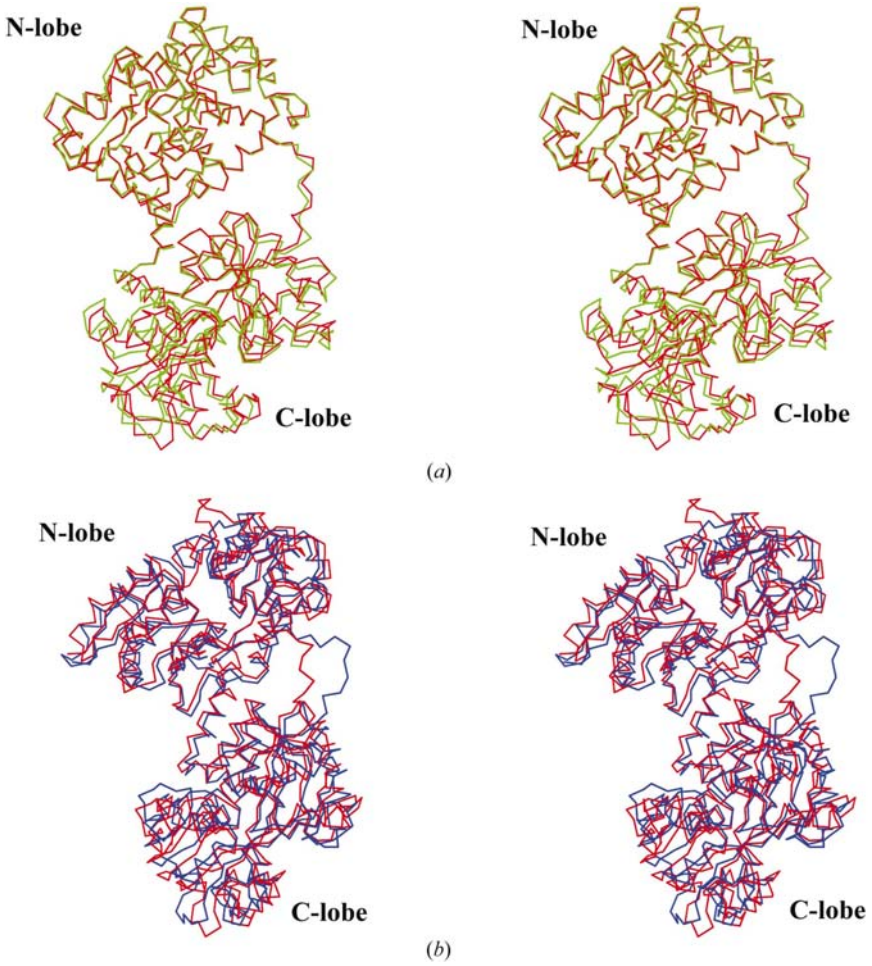


**Figure 5**
Structural comparison of serum transferrin and ovotransferrin. Stereoviews of the superposition of $C^{\alpha}$ traces on the basis of N lobes showing the altered orientation of the two lobes in hen serum transferrin (red) compared with (*a*) hen ovotransferrin (green) and (*b*) rabbit serum transferrin (blue).

## 4. Conclusion

The present structure of diferric hen serum transferrin at 2.8 Å reveals that the overall fold of the polypeptide chain is similar to other members of the transferrin family. The type of interactions observed in the hST structure have more resemblance to those of other serum transferrins than those of ovotransferrins or lactoferrins. On the basis of the intralobe and interlobe interactions and the presence of a possible second carbohydrate-attachment site, it can be suggested that both the lobes of hST are more stable compared with those of hOT. This may modulate its iron-binding/release property, which is related to its iron-trans-

port function. The difference in the orientations of both the lobes of hST with respect to ovotransferrin, serum transferrin and lactoferrin can be correlated with the species-specific receptor-recognition property of this class of proteins.

We wish to thank Abhijit Bhattacharyya for help in preparing the illustrations and Bikram Nath for help during purification and crystallization.

## References


Aisen, P. (1989). *Iron Carriers and Iron Proteins*, edited by T. Loeler, pp. 353–371, New York: VCH.

Bailey, S., Evans, R. W., Garratt, R. C., Gorinsky, B., Hasnain, S., Horsburgh, C., Jhoti, H., Lindley, P. F., Mydin, A., Sarra, R. & Watson, J. L. (1988). *Biochemistry*, **27**, 5804–5812.

Baker, E. N. & Lindley, P. F. (1992). *Inorg. Biochem.* **47**, 147–160.

Baker, E. N. (1994). *Adv. Org. Chem.* **41**, 389–463.

Bewley, M. C., Tam, B. M., Grewal, J., He, S., Shewry, S., Murphy, M. E. P., Mason, A. B., Woodworth, R. C., Baker, E. N. & MacGillivray, R. T. A. (1999). *Biochemistry*, **38**, 2535–2541.

Brünger, A. T., Adams, P. D., Clore, G. M., DeLano, W. L., Gros, P., Grosse-Kunstleve, R. W., Jiang, J.-S., Kuszewski, J., Nilges, M., Pannu, N. S., Read, R. J., Rice, L. M., Simonson, T. & Warren, G. L. (1998). *Acta Cryst.* D**54**, 905–921.

Brünger, A. T., Karplus, M. & Petsko, G. A. (1989). *Acta Cryst.* A**45**, 50–61.

Choudhury, D., Guha Thakurta, P., Dasgupta, R., Sen, U., Biswas, S., Chakrabarti, C. & Dattagupta, J. K. (2002). *Biochem. Biophys. Res. Commun.* **295**, 125–128.

Collaborative Computational Project, Number 4 (1994). *Acta Cryst.* D**50**, 760–763.

Dautry-Varsat, A., Cienchanover, A. & Lodish, H. F. (1983). *Proc. Natl Acad. Sci. USA*, **80**, 2258–2262.

Dewan, J. C., Mikami, B., Hirose, M. & Sacchettini, J. C. (1993). *Biochemistry*, **32**, 11963–11968.

El Hage Chahine, J. M. & Pakdaman, R. (1975). *Eur. J. Biochem.* **230**, 1101–1110.

Esnouf, R. M. (1997). *J. Mol. Graph.* **15**, 132–134.

Grossmann, G. J., New, M., Pantos, E., Schwab, F. J., Evans, R. W., Townes-Andrews, E., Lindley, P. F., Appel, H., Thies, W. G. & Hasnain, S. S. (1991). *J. Mol. Biol.* **231**, 554–558.

Hall, D. R., Hadden, J. M., Leonard, G. A., Bailey, S., Neu, M., Winn, M. & Lindley, P. F. (2002). *Acta Cryst.* D**58**, 70–80.

Haridas, M., Anderson, B. F. & Baker, E. N. (1995). *Acta Cryst.* D**51**, 629–646.

Jameson, G. B., Anderson, B. F., Norris, G. E., Thomas, D. H. & Baker, E. N. (1998). *Acta Cryst.* D**54**, 1319–1335.

Jeffrey, P. D., Bewley, M. C., MacGillvray, R. T. A., Mason, A. B., Woodworth, R. C. & Baker, E. N. (1998). *Biochemistry*, **37**, 13978–13986.

Jones, T. A., Zou, J. Y., Cowan, S. W. & Kjeldgaard, M. (1991). *Acta Cryst.* A**47**, 110–119.

Karthikeyan, S., Paramasivam, M., Yadav, S., Srinivasan, A. & Singh T. P. (1999). *Acta Cryst.* D**55**, 1805–1813.

Khan, J. A, Kumar, P., Paramasivam, M., Yadav, R. S., Sahani, M. S., Sharma, S., Srinivasan, A. & Singh, T. P. (2001). *J. Mol. Biol.* **309**, 751–761.

Kleywegt, G. J. & Jones, T. A. (1998). *Acta Cryst.* D**54**, 1119–1131.

Kraulis, P. J. (1991). *J. Appl. Cryst.* **24**, 946–950.

Kurokawa, H., Dewan, J. C., Mikami, B., Sacchettini, J. C. & Hirose, M. (1999). *J. Biol. Chem.* **274**, 28445–28452.

Kurokawa, H., Mikami, B. & Hirose, M. (1995). *J. Mol. Biol.* **254**, 196–207.

Kuser, P., Hall, D. R., Haw, M. L., Neu, M., Evans, R. W. & Lindley, P. F. (2002). *Acta Cryst.* D**58**, 777–783.

Laskowski, R. A., MacArthur, M. W., Moss, D. S. & Thornton, J. M. (1993). *J. Appl. Cryst.* **26**, 283–291.

Lin, L. N., Mason, A. B., Woodworth, R. C. & Brandts, J. F. (1991). *Biochemistry*, **30**, 11660–11669.

Lindley, P. F., Bajaj, M., Evans, R. W., Garratt, R. C., Hasnain, S. S., Jhoti, H., Kuser, P., Neu, M., Patel, K., Sarra, R., Strange, P. & Walton, A. (1993). *Acta Cryst.* D**49**, 292–304.

MacGillivray, R. T. A., Bewley, M. C., Smith, C. A., He, Q. Y., Mason, A. B., Woodworth, R. C. & Baker, E. N. (2000). *Biochemistry*, **39**, 1211–1216.

MacGillivray, R. T. A., Moore, S. A., Chen, J., Anderson, B. F., Baker, H., Luo, Y., Bewley, M., Smith, C. A., Murphy, M. E. P., Wang, Y., Mason, A. B., Woodworth, R. C., Brayer, J. D. & Baker, E. N. (1998). *Biochemistry*, **37**, 7919–7928.

Mason, A. B., Brown, S. A. & Church, W. R. (1987). *J. Biol. Chem.* **262**, 9011–9015.

Mason, A. B., Tam, B. M., Woodworth, R. C., Oliver, R. W. A., Green, B. N., Lin, L.-N., Brandts, J. F., Savage, K. J., Lineback, J. A. & MacGillivray, R. T. A. (1997). *Biochem. J.* **326**, 77–85.

Mason, A. B. & Woodworth, R. C. (1984). *J. Biol. Chem.* **259**, 1866–1873.

Mason, A. B., Woodworth, R. C., Oliver, R. W. A., Green, B. N., Lin, L.-N., Brandts, J. F., Savage, K. J., Tam, B. M. & MacGillivray, R. T. A. (1996). *Biochem. J.* **319**, 361–368.

Mer, G., Hietter, H. & Lefévre, J.-F. (1996). *Nature Struct. Biol.* **3**, 45–53.

Mizutani, K., Mikami, B. & Hirose, M. (2001). *J. Mol. Biol.* **309**, 937–947.

Mizutani, K., Muralidhara, B. K., Yamashita, H., Tabeta, S., Mikami, B. & Hirose, M. (2001). *J. Biol. Chem.* **276**, 35940–35946.

Mizutani, K., Yamashita, H., Kurokawa, H., Mikami, B. & Hirose, M. (1999). *J. Biol. Chem.* **274**, 10190–10194.

Mizutani, K., Yamashita, H., Mikami, B. & Hirose, M. (2000). *Biochemistry*, **39**, 3258–3265.

Montreuil, J., Tonnelat, J. & Mullet, S. (1960). *Biochim. Biophys. Acta*, **45**, 413–421.

Moore, S. A., Anderson, B. F., Groom, C. R., Haridas, M. & Baker, E. N. (1997). *J. Mol. Biol.* **274**, 222–236.

Navaza, J. (1994). *Acta Cryst.* A**50**, 157–163.

Nurizzo, B., Baker, H. M., He, Q.-Y., MacGillivray, R. T. A., Mason, A. B., Woodworth, R. C. & Baker, E. N. (2001). *Biochemistry*, **40**, 1616–1623.

Otwinowski, Z. & Minor, W. (1997). *Methods Enzymol.* **276**, 307–326.

Rawas, A., Moreton, K., Muirhead, H. & Williams, J. (1989). *J. Mol. Biol.* **208**, 213–214.

Rawas, A., Muirhead, H. & Williams, J. (1996). *Acta Cryst.* D**52**, 631–640.

Rudd, P. M., Joao, H. C., Coghill, E., Fiten, P., Saunders, M. R., Opdenakker, G. & Dwek, R. A. (1994). *Biochemistry*, **33**, 17–22.

Sharma, A. K., Paramasivam, M., Srinivasan, A., Yadav, M. P. & Singh, T. P. (1999). *J. Mol. Biol.* **289**, 303–317.

Sharma, A. K., Rajashankar, K. R., Yadav, M. P. & Singh, T. P. (1999). *Acta Cryst.* D**55**, 1152–1157.

Shimo-oka, T., Hagiwara, Y. & Ozawa, E. (1986). *J. Cell. Physiol.* **126**, 341–351.

Thibodeau, S. N., Lee, D. C. & Palmiter, R. D. (1978). *J. Biol. Chem.* **253**, 3771–3774.

Wang, C., Eufemi, M., Turano, C. & Giartosio, A. (1996). *Biochemistry*, **35**, 7299–7307.

Williams, J. (1968). *Biochem. J.* **108**, 57–67.

Williams, J. & Moreton, K. (1988). *Biochem. J.* **251**, 849–855.

Woodworth, R. C., Mason, A. B., Funk, W. D. & MacGillivray, R. T. A. (1991). *Biochemistry*, **30**, 10825–10829.

Young, S. P., Bomford, A. & Williams, R. (1984). *Biochem. J.* **219**, 505–510.